Wireless Power Transmission in the SmartHome

by

YIN QUAN TEO
Advisor: DR. MATTHEW S. REYNOLDS

Department of Electrical and Computer Engineering
Duke University

Abstract

WE DEVELOP A wireless power transmission system for the Duke SmartHome. This power-transmitting surface is built into the frame of a 35 x 32 cm wooden cabinet and is able to transmit tens of watts of electrical power to power multiple devices simultaneously. We have successfully powered multiple devices including an alarm clock, a USB light, an LED, a USB toy and an iPhone. We have also managed to power 4 iPhones simultaneously.

Existing techniques of wireless power transmission involving a pair of strongly magnetically coupled resonators allow transmission of tens of watts of power over a few meters [4]. By introducing high Q L-C resonators, researchers are able to efficiently transfer power from one resonant transmitter to another resonant receiver. However, efficiency greatly deteriorates upon adding more receivers to the strongly coupled system because of the interactions between multiple coupled resonators.

We observe that many consumer electronics for example laptops, desk lamps, alarm clocks etc operate off a surface such as a desk or a cabinet. In our research and implementation of a wireless power transmission system, we transmit near field wireless power with a goal not to maximize the distance of power transmission, but rather, to power devices on a surface. Our objective is to allow the introduction of numerous non-resonant pick up coils to enable multiple devices to be powered on the surface at once with only one resonant transmitter.

With the goal of powering multiple devices with a single transmitter, we design a system that drives a primary inductor that is coupled with a high Q L-C secondary resonator. Design parameters such as drive frequency, number of turns of resonant coil, type of wire used etc are determined by computer modeling. MATLAB is used to model the behavior of inductive power transfer and PSpice is used to model the behavior of the transmitter and receiving systems respectively.

Table of Contents

1 Introduction

1.1 Related Work

The first visions of wireless power transmission came from Nikola Tesla in the early 20th century [1], [2]. His biggest project involved the Wardenclyffe Tower. Although the transmitting tower could be used for wireless communications, it was constructed with the intention to transmit wireless power [3]. In Tesla's power transmission system, he hypothesized the Earth to be a giant charged sphere that could be driven at its resonant frequency and that he could close the circuit using giant electric fields in the Earth's ionosphere [1]. Much of his research on wireless power involved radiative electromagnetic waves that are practical for transferring information but pose immense difficulties for wireless power transfer for two reasons [4]. Firstly, omnidirectional radiation is very power inefficient. Secondly, if we were to use unidirectional radiation instead, we would require a direct line of sight and complicated tracking mechanisms.

Although wireless power could have been developed a lot earlier, there was never strong demand for it because of the lack of mobile electronic devices then. Commonplace mobile electronics today such as laptops and cellphones have caused a renewed interest in wireless power [5], [6], [7]. In 2007, a group of researchers at MIT achieved wireless power transfer, powering a light bulb of 60W over distances exceeding 2 meters with efficiency of around 40% [4]. In their wireless power system, they use a pair of strongly magnetically coupled resonators, with a transmitter and a receiver forming a resonant pair.

A lot of research since then ([4], [11], [12]) has focused on a resonant transmitter and receiver pair to transfer power wirelessly. Such an architecture has a highly efficient one to one coupling between the resonant transmitter and receiver. However, adding more receivers causes the efficiency of power transfer to deteriorate tremendously.

1.2 Motivation and Project Goals

The motivation for wireless power comes from wires being cumbersome and messy. With the large number of mobile electronics that we own today, there is a demand for convenience in managing their power supplies. Wireless communication has revolutionized the way we interact with communication devices. In a world without wireless communication, we would have to go through the cumbersome process of locating an Ethernet port and then connecting our device to it via a cable before gaining access to the Internet. We are well aware of the convenience that wireless communication brings to us and wireless power will add to that convenience tremendously.

We next observe that many consumer electronics for example laptops, desk lamps, alarm clocks etc operate off a surface such as a desk or a cabinet. Hence, unlike the research in [4], our goal is not to maximize the distance of power transmission, but rather, to design a surface for near field wireless power transfer. This is ideal since most electronic devices have to be operated off a surface.

We also observe that while the techniques of strongly coupled magnetic resonances allow efficient power transfer between a pair of transmitter and receiver coils, efficiency greatly deteriorates upon adding more receivers to the strongly coupled system due to the interaction between multiple coupled resonators. In tightly coupled resonant wireless power transfer, we require a one to one correspondence between transmitter and receiver. This system then is not scalable for a large number of users with a large number of mobile devices because every single device has to have its own unique transmitter. A hypothetical conference room providing wireless power to laptop computers for twenty users will have to have 20 transmitters and each of the users will have to pre-tune their receivers to the right frequency. With this in mind, the goal of our work is to allow the powering of multiple devices with only one resonant transmitter through the introduction of numerous non-resonant pick up coils. We design these non-resonant pick up coils to power generic USB devices.

In addition, in order to improve efficiency of power transfer, we aim to use a lower switching frequency to drive the gate of our MOSFET. In the resonant coupled system in [4], a drive frequency of 10 MHz was used. We aim to use a drive frequency in the kHz range in order to improve the efficiency of switching and reduce the heat dissipated in the MOSFET.

2 Inductive Power Transfer Principles

2.1 Model Derivation

In our power surface design, we deal with coupled rectangular coils. It is then useful to model the behavior of coupled rectangular coils using the physics behind inductive power transfer [8], [9].

Applying Bio-Savart's Law, it can be shown [9] that the magnetic flux density at a point at a distance r from a straight conductor (Fig 1) making an angle of θ_1 with one end and an angle of θ_2 with the other end and having a current I flowing through the conductor is given by

$$B = \frac{\mu_0 I}{4\pi r}(\sin\theta_2 - \sin\theta_1) \quad \textbf{(1)}$$

where $\mu_0 = 4\pi$ x 10^{-7} H/m.

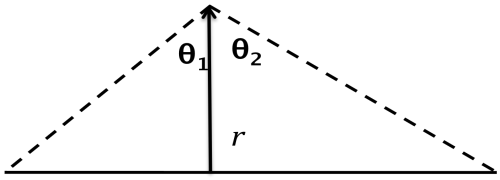

Figure 1: A point at a distance *r* from a straight conductor.

Setting the origin (0,0) to be the bottom left of a coil of wire, we can calculate the magnetic flux density at a point (x,y) within a coil of dimensions *a* x *b* m by taking the superposition of the magnetic flux density due to each of the four individual straight conductors that make up the rectangular coil of wire. (Fig 2)

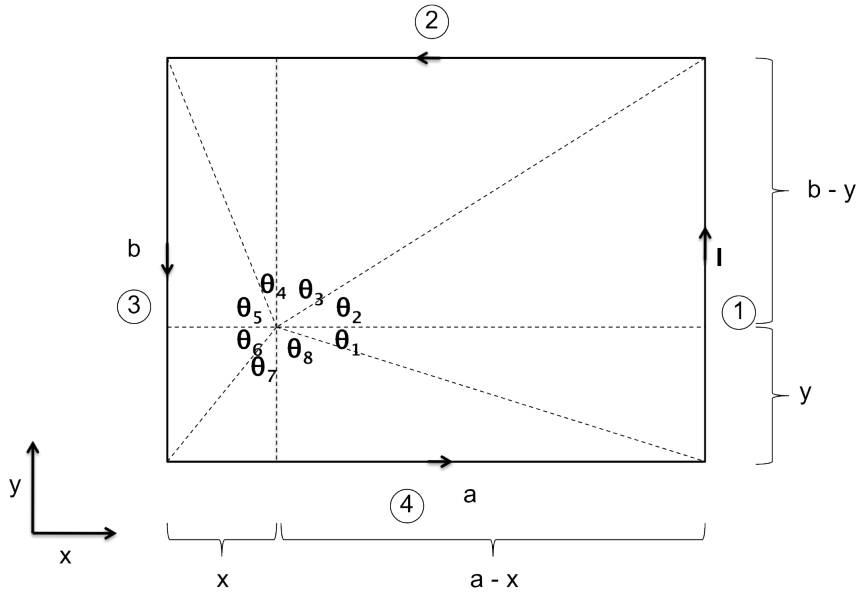

Figure 2: Four individual straight wires making up a rectangular coil.

From figure 2, the magnetic flux density at (x,y), where l_i is the perpendicular distance from (x,y) to segment *i* of the rectangular coil is given by

$$B = \frac{\mu_0 I N_{tx}}{4\pi} \sum_{i=1}^{4} \frac{1}{l_i} (\sin\theta_{2i} - \sin\theta_{2i-1}) \qquad \textbf{(2)}$$

where N_{tx} is the number of turns of the transmitting coil and we have made the assumption that each turn of wire has negligible height and are stacked directly on top of one another.

In our power surface, the current in our transmitting coil varies with time and can be written as $I_{tx} = I \sin(\omega t)$. For a rectangular receiving coil of dimensions a_0 x b_0 m that is placed on top of the transmitting coil, we can obtain the magnetic flux through the receiving coil by integrating the magnetic flux density **B**, over all points within the a_0 x b_0 coil,

$$\Phi = \iint \vec{B}(x,y,t) \cdot d\vec{A} \tag{3}$$

The changing magnetic flux induces an electric potential given by Faraday's law. Taking the time derivative of equation 3 and scaling the induced voltage by the number of turns N_{rx} on the receiving coil, we obtain the open circuit peak voltage across the receiving coil:

$$|\varepsilon| = \frac{\omega \mu_0 N_{tx} N_{rx} I}{4\pi} \bullet \int_{y_0}^{y_0+b_0} \int_{x_0}^{x_0+a_0} \left\{ \begin{array}{l} \frac{1}{a-x}\left[\frac{b-y}{\sqrt{(a-x)^2+(b-y)^2}} + \frac{y}{\sqrt{(a-x)^2+y^2}}\right] \\ + \frac{1}{b-y}\left[\frac{x}{\sqrt{x^2+(b-y)^2}} + \frac{a-x}{\sqrt{(a-x)^2+(b-y)^2}}\right] \\ + \frac{1}{x}\left[\frac{y}{\sqrt{x^2+y^2}} + \frac{b-y}{\sqrt{x^2+(b-y)^2}}\right] \\ + \frac{1}{y}\left[\frac{x}{\sqrt{x^2+y^2}} + \frac{a-x}{\sqrt{(a-x)^2+y^2}}\right]\right) dxdy \end{array} \right\} \tag{4}$$

where (x_0, y_0) refers to the coordinates of the bottom left corner of the receiving coil with respect to the transmitting coil.

2.2 MATLAB Model

Equation 4 is the basis of our model for inductively coupled rectangular coils. We implement this equation in MATLAB to obtain numerical values for the induced electric potential across a receiving coil. To test our model, we obtain empirical values that we will use to compare against the output of our MATLAB model.

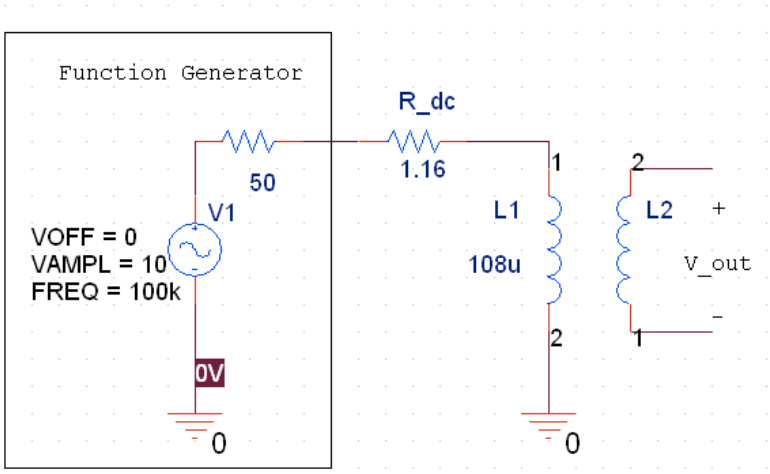

Fig 3. Experimental set up to examine inductive coupling.

We use a function generator to drive a 15.3 x 9.67 cm transmitting coil of 20 turns (Fig 3) at 20 V_{pp} and 100 kHz. Using receiving coils of various dimensions and number of turns, we place them as close to the edge of the transmitting coil as possible and then measure the open circuit voltage induced. Ideally, the wires in both the transmitter and receiver will be stacked directly on top of each other, with the wires taking up negligible width. However, the physical coils of wire take up significant width when coiled up (Fig 4). Taking measurements from the centroid of each edge, the average separation between the transmitting and receiving coil is 8mm.

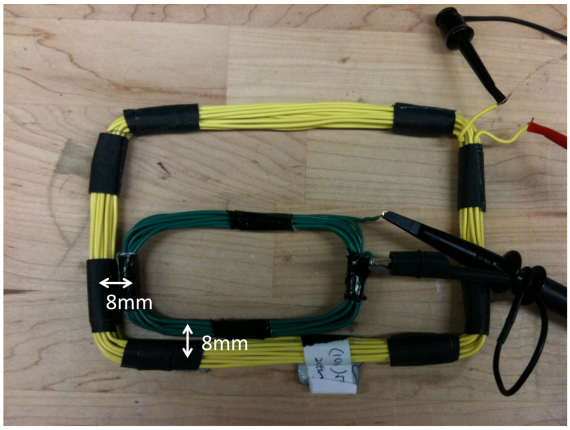

Fig 4. Separation distance due to physical width of wires

Based on the physical dimensions, placement of the coils and the transmitter frequency, we have all the input parameters to our model except for the current in the primary coil. We measure the self-inductance of the primary coil to be 108μH and its DC resistance to be 1.16Ω. Using PSpice (Fig 5), we obtain the drive current in the primary coil to be $220mA_{pp}$.

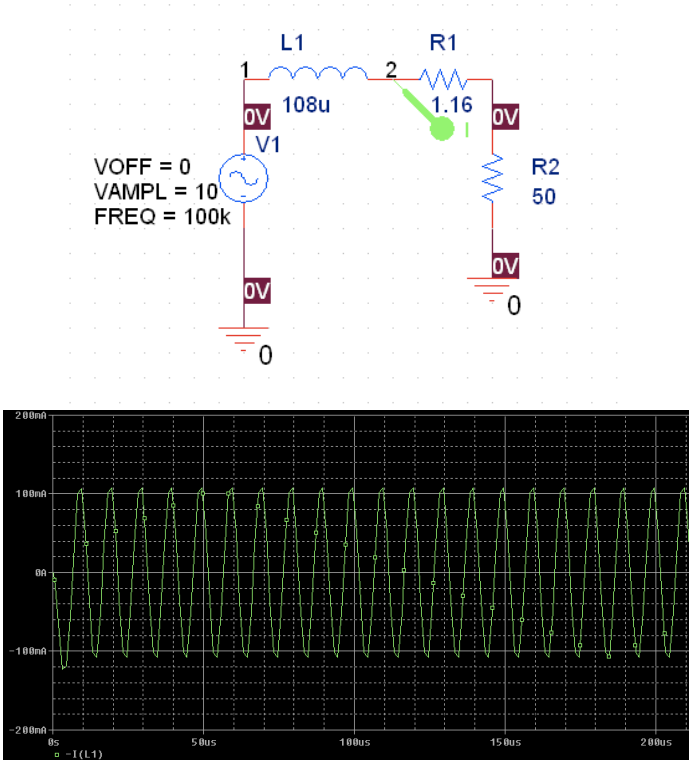

Fig 5. PSpice drive coil set up and current probe reading. (top to bottom)

Using these input parameters, we can obtain the induced open circuit voltage with our MATLAB model. The results of our comparison with the empirically measured induced voltages are shown in Table 1 below.

Dimensions (cm x cm)	**No. Turns**	**Voltage Measured (V_{pp})**	**Voltage Computer Model (V_{pp})**	**Error (%)**
10.70 x 6.40	20	5.55	5.36	3.4
10.89 x 6.30	10	2.64	2.69	1.9
7.26 x 4.15	7	0.940	0.918	2.3
10.88 x 6.53	5	1.50	1.39	7.3
9.36 x 4.94	5	0.940	0.940	0.0
8.47 x 4.62	10	1.66	1.63	1.8
9.25 x 4.29	12	2.00	1.99	0.5

Table 1: Comparing the measured open circuit induced voltages with values predicted by the MATLAB model for different transmitting and receiving coils.

Comparing our results, our MATLAB model predicts fairly accurately the empirically measured induced voltage across receiving coils of various dimensions and number of turns. The errors are due to the following reasons: (1) Non uniform dimension of coils, i.e. our coils are not perfect rectangles. (2) Wires not stacked up directly on top of each other and not having infinitesimally small widths. Note that the errors could be mitigated by placing the secondary coil at the center of a primary coil with dimensions that are much greater compared to the secondary coil. This is because of a much more uniform magnetic flux density in the center of a large transmitter coil.

3 Wireless Power Transmission System

3.1 Operating Principles

The principles of operation of our wireless transmission system are very similar to the surface based wireless power transmission system used for communication within robot swarms [10].

In a resonant system, the circulating current in the resonant coil is greater than the drive

coil by the quality factor Q. We use a drive circuit to switch a power MOSFET at our desired transmission frequency (Fig 6).

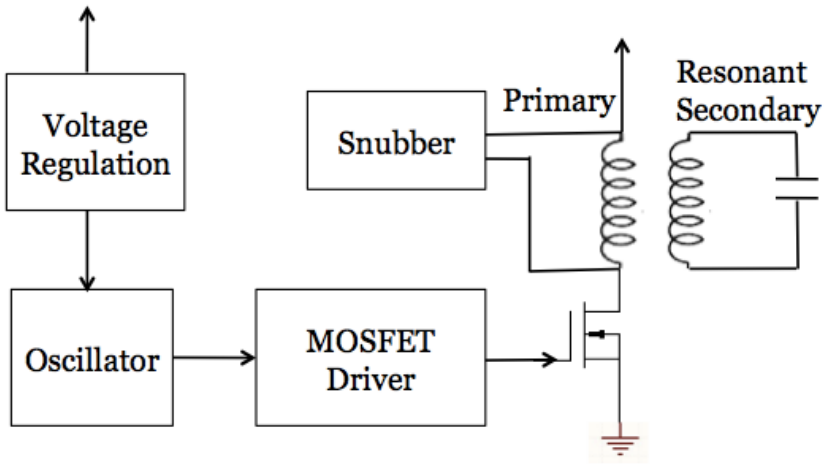

Fig 6. Block diagram of power surface transmitter.

A time varying current flows in a primary drive coil that is coupled with a resonant LC secondary coil. Current is induced in our secondary coil at the transmission frequency, which we want to set as our resonance frequency. The resonant frequency of the secondary coil can be calculated from the inductance and capacitance of the LC circuit,

$$f_{res} = \frac{1}{2\pi\sqrt{LC}} \tag{5}$$

To power multiple devices without altering the resonant frequency of the system, we use multiple non-resonant pick up coils in our receivers. The modeling of the behavior of non-resonant coupling has been discussed at great lengths in Section 2 Inductive Power Transfer Principles.

Because of the high magnetic flux density as a result of our resonant coil, we can design the receivers to sit on a surface that separates the transmitter and receivers by a certain distance. This is unlike a non-resonant transformer system such as an inductive toothbrush charger where the receiving coil has to be placed within the protruding transmitter coil for maximum coupling.

In designing the receivers, we know that the current flowing in the resonant coil is greater than Q compared to the drive current in the primary coil. This allows us to

calculate the open voltage induced across a non-resonant pick up coil of dimensions a_0 x b_0 m with N_{rx} turns using the computer model in section 2.1 (equation 4). We can control in our resonant transmitter coil, the number of turns N_{tx} and its dimensions a x b m. The only unknown quantity then is the current in our resonant coil, which we can then calculate from the current flowing in our primary drive coil and the Q factor.

3.2 PSpice Model

In order to aid us in the design of our transmitter, we use PSpice (Fig 7) to model the behavior of our transmitter.

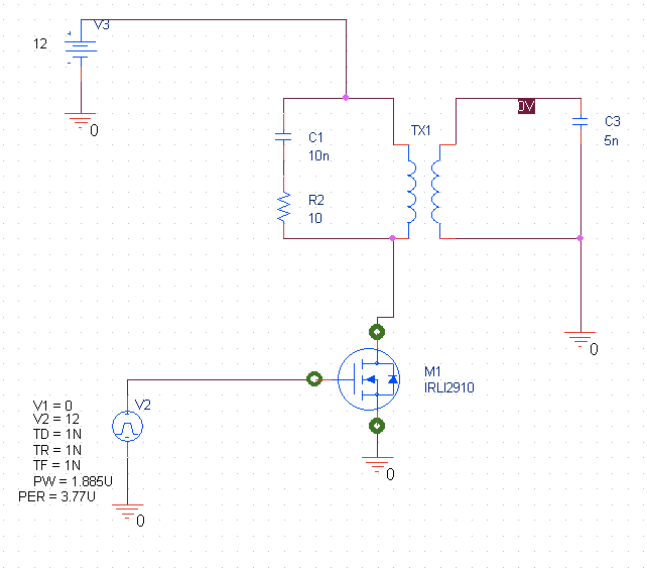

Figure 7: Driver circuit model

Our PSpice model helps us in the design of our transmitter by allowing us to observe the behavior of our system as we tweak design parameters such as the drive frequency at the gate of the MOSFET or the number of turns within the resonant coil or the values of our passive components in the snubber.

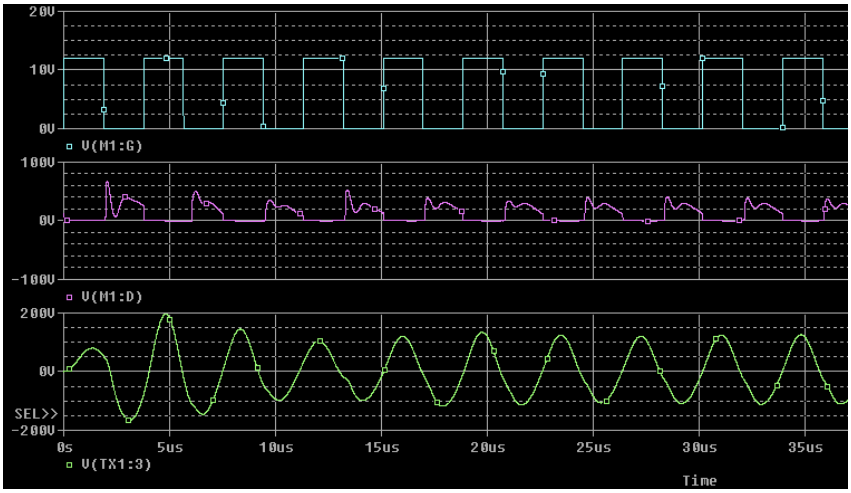

Figure 8: From top to bottom - Input to gate of MOSFET. Drain of MOSFET. Voltage across resonant coil. (PSpice Model)

Using PSpice, we can look at the voltage at the gate and drain of our MOSFET, the voltage across the resonant coil and the current flowing through our primary and resonant coil. Fig 8 shows some of these waveforms with a 9 turn-resonant coil of inductance 72 μH in parallel with a 5 nF capacitor being driven at its resonance frequency of 265 kHz. We obtain the value of inductance by physically constructing the resonant coil and measuring its inductance with an LCR meter.

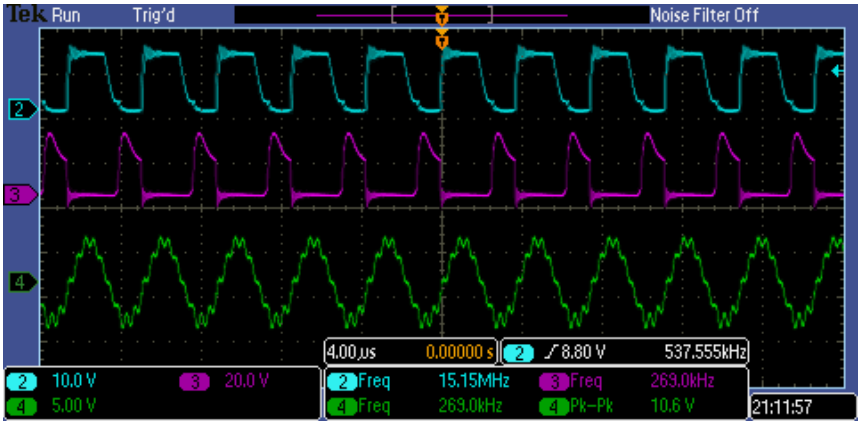

Figure 9: From top to bottom - Input to gate of MOSFET. Drain of MOSFET. Voltage across test coil. (Oscilloscope measurements)

After constructing the coil (refer to 4.1 Transmitter Design), we compare the waveforms we obtained from PSpice with an oscilloscope and notice the similarity. The PSpice model suffers the shortcoming of not capturing the slew rate at the gate of our MOSFET. Despite that, we see consistent waveforms with accurate peak voltages. Thus, our PSpice model provides a good model for the behavior of our transmitter system.

4 Wireless Power System Design

4.1 Transmitter Design

Driving the power MOSFET at high frequencies causes excessive power loss and reduced efficiency. To minimize the transient power loss due to switching, we have chosen to drive the MOSFET in the kHz range (~250kHz). Our resonant coil has to tolerate large currents. As such, we choose mica capacitors in our resonant coil as they have excellent thermal stability, high Q and low power loss. We choose the capacitance in our resonant coil to be 5 nF. Using equation 5, we require an inductance of 81 μH in our resonant coil.

The power surface of choice for our prototype is a small wooden cabinet that can fit a resonating coil of dimensions 34.6 x 31.75 cm. 9 turns on the resonant coil with 14 AWG wire gives us a self-inductance of 72 μH. Based on the new value of inductance, the resonance frequency of the resonant coil is 265.2 kHz.

We measure the DC resistance of the resonant coil to be 0.86 Ω. The calculated coil Q based on

$$Q = \frac{2\pi fL}{R} \tag{6}$$

is Q = 140 discounting skin effect and dielectric losses.

To measure the actual Q of the coil, we drive the transmitting coil at various frequencies with a function generator generating a $20V_{pp}$ AC output and measure the induced voltage across a 10 x 6 cm, 20 turn test coil placed in the center of the transmitting coil. The results are shown in Fig 10.

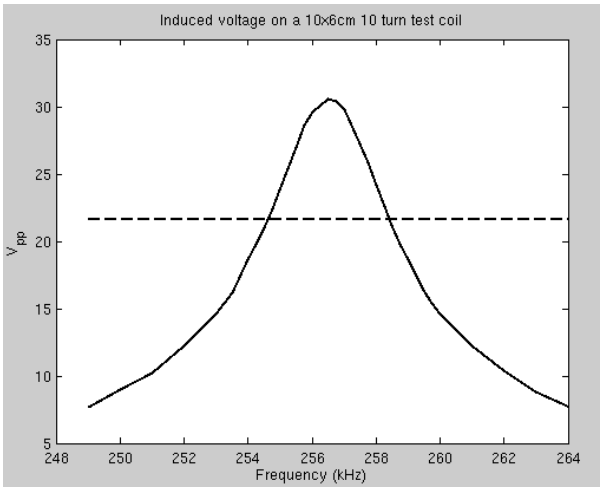

Fig 10. Calculating Q from the induced voltages across test coils picking up magnetic flux from the transmitting coil, driven at various frequencies.

The bandwidth of the coil Δf is the difference in the frequencies where we get a half power response from the resonant coil. From the results in Fig 10, we can calculate Q experimentally using

$$Q = \frac{f_{res}}{\Delta f} \tag{7}$$

which gives us a value of Q = 67.4. The difference in Q is due to the power losses in the mica capacitors in our resonant coil and materials near to the transmitting coil.

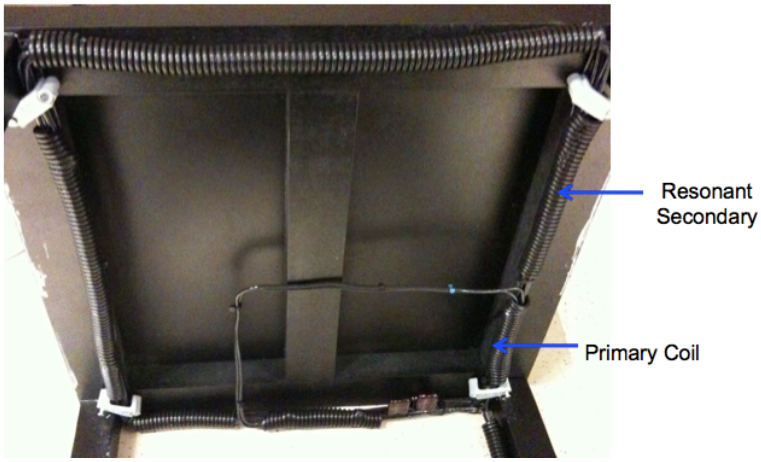

Fig 11. Coupling between primary and resonant coil.

Fig 11 shows the set up of our primary and resonant coil. The primary coil is about a sixth of the area of the secondary in order to reduce its coupling with the other non-resonant receivers and also to reduce its self-inductance.

Figure 12 shows the magnetic flux density across the wooden cabinet that we use to house the primary and resonant coil using the MATLAB model from earlier. The magnetic flux density is plotted on a negative scale in order to show the relative uniform field of around 50 Gauss within the center of the table.

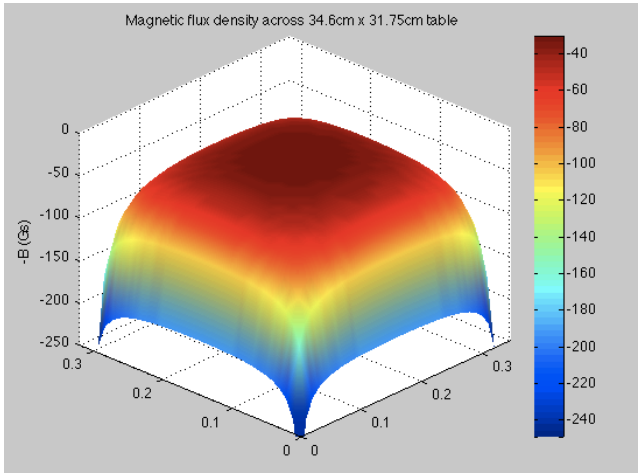

Fig 12. Magnetic flux density across surface of wooden cabinet.

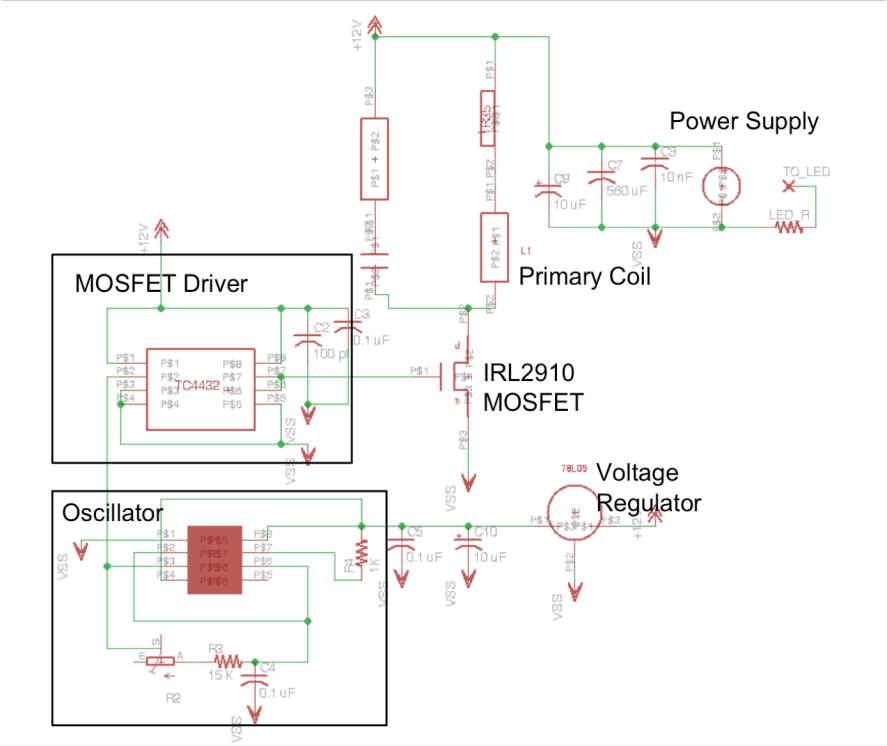

Fig 13: Circuit design of drive circuitry.

In our drive circuitry, it is important to have a stable power supply to the oscillator. An unstable power supply due to either transients in placing pickup coils or due to the switching on of the power supply alters the frequency of the output square wave at the oscillator in unpredictable ways. This behavior can result in a feedback system – affecting the drive frequency of the primary coil, which then affects the current drawn in the power supply, and ultimately altering the frequency of the output square wave at the oscillator. We solve this problem by regulating power supply to the oscillator.

Fig 14: PCB of drive circuitry.

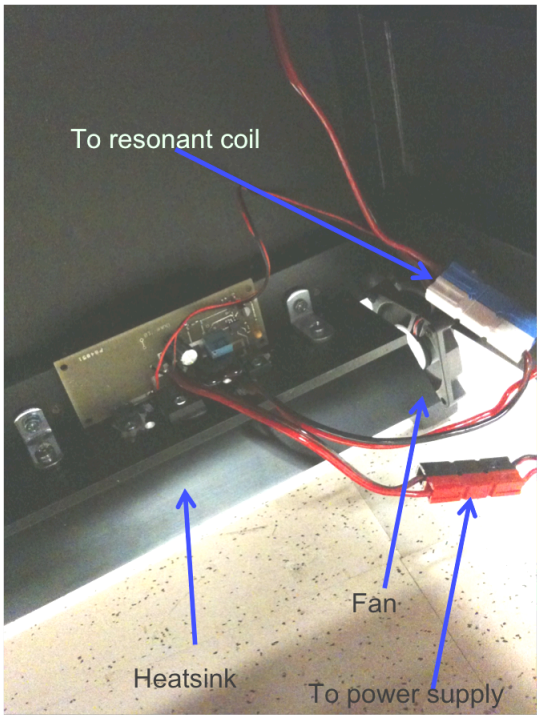

Fig 15: Drive circuitry mounted to heat sink with a cooling fan.

The drive circuitry is shown in figures 14 and 15. Thermal cooling of the snubber resistor and FET is important because of high dissipation of thermal energy. We have attached the drive PCB to a heatsink and installed a 12V cooling fan to cool our drive circuitry.

4.2 Receiver Design

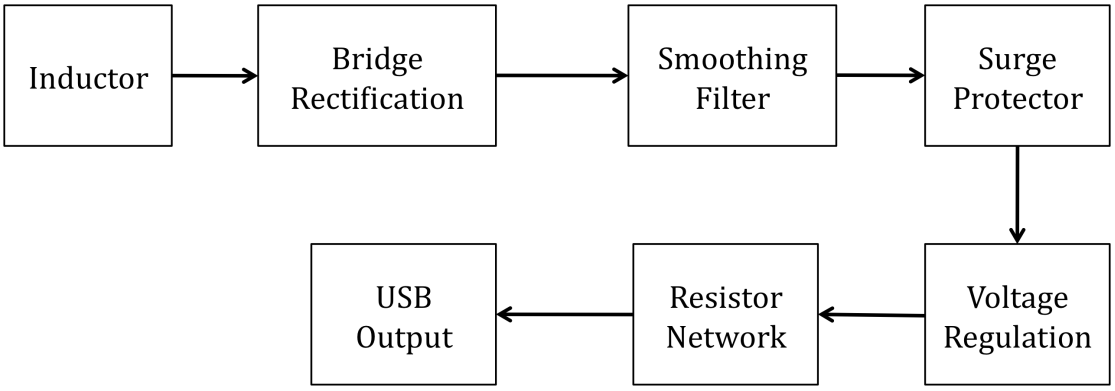

Fig 16: Receiver block diagram.

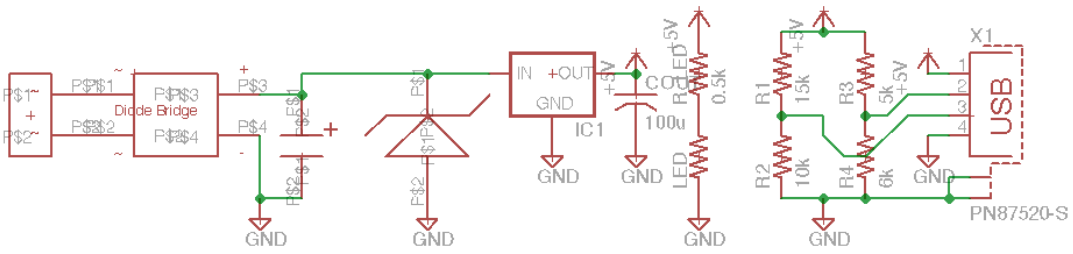

Fig 17: Receiver circuitry.

We design our receiver (fig 16 and 17) to power generic USB devices. A diode bridge is used for full wave rectification. A smoothing capacitor is used to smoothen the peak voltages and a zener diode is added to at the output of the bridge to protect the load from voltage spikes. The resistor network is added in order to provide a 2V to D+ and

~2.7V to D-, where D+ and D- are the + and – data pins on the USB output. This resistor network allows the charging of Apple devices such as iPod touches and iPhones.

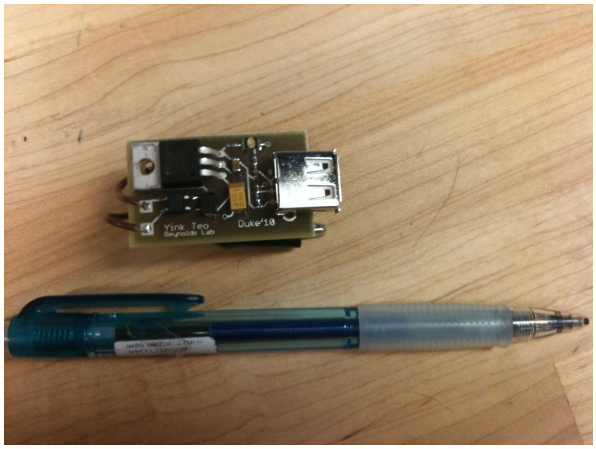

Fig 18: PCB of receiver.

5 Efficiency

Counter-intuitively, our power surface becomes more efficient as we increase the number of devices drawing power from it (Table 2). The efficiency we are considering is the ratio of the power consumed by the power supply to the power provided to the devices we are powering on the power surface. We have considered the efficiency from converting from a DC power source to AC magnetic field and from an AC induced voltage to a DC output. This is unlike the AC to AC metric used in [4].

Number of iPhones	Total DC to DC Transfer Efficiency (%)
1	5
2	11
3	20
4	33

Table 2: Efficiency of power surface with different number of devices on it

Our efficiency increases when more devices are placed on the power surface because more of the magnetic field on the power surface is being captured.

Conclusion

We have successfully implemented a power surface with a low frequency drive that is able to power multiple devices. This power surface prototype is built into a 35 x 32 cm wooden cabinet and consists of a single resonant transmitter that provides power to multiple non-resonant receivers. We have built a receiver that powers generic USB devices and have shown that we can power 4 Apple iPhones simultaneously with our power surface. The total efficiency increases with the number of devices that we place on the power surface.

Fig 19: Power surface prototype powering multiple devices

Acknowledgements

I like to thank my advisor, Dr. Matthew Reynolds, for guiding my research and providing valuable insight and advice. I like to thank graduate student Stewart Thomas for his guidance on how to use the EAGLE CAD circuit design software. Lastly, I like to thank Martha Absher for the Pratt Fellows Program and the opportunity to conduct intensive graduate level research as an undergraduate.

References

[1] Tesla, Nikola, "The True Wireless". Electrical Experimenter, May 1919

[2] N. Tesla, U.S. patent 1,119,732 (1914)

[3] Nikola Tesla, "The Transmission of Electrical Energy Without Wires as a Means for furthering Peace," *Electrical World and Engineer*. Jan. 7, p. 21, 1905.

[4] A. Kurs *et al.*, "Wireless Power Transfer via Strongly Coupled Magnetic Resonances" in *Science* **317** (5834), 83. 6 July 2007.

[5] B. Wells, U.S patent 6,972,543 (2005)

[6] H. Mita, U.S patent 2010/0052431 A1 (2010)

[7] A. Machinsky, International patent WO 2010/024895 A1 (2010)

[8] K. Finkenzeller. RFID Handbook: Fundamentals and Applications in Contactless Smart Cards and Identification. Wiley, 2003.

[9] J. Jewett and R. Serway. Physics for scientists and engineers with modern physics. pg 840 Brooks/Cole, 2007.

[10] T. Deyle and M. Reynolds, "Surface based wireless power transmission and bidirectional communication for autonomous robot swarms" in Proceedings IEEE Conference on Robotics and Automation 2008, pp. 1036-1041. May 2008.

[11] J. Taylor, Z.N. Low; J. Casanova, J. Lin, "A wireless power station for laptop computers," *Radio and Wireless Symposium (RWS), 2010 IEEE* , vol., no., pp.625-628, 10-14 Jan. 2010

[12] P. Sample, T. Meyer, J. Smith, "Analysis, Experimental Results, and Range Adaptation of Magnetically Coupled Resonators for Wireless Power Transfer," *Industrial Electronics, IEEE Transactions on* , vol.PP, no.99, pp.1-1, 0 doi: 10.1109/TIE.2010.2046002